View metadata, citation and similar papers at core.ac.uk
brought to you by CORE
provided by PolyU Institutional Repository

Modeling of Solenoidal Transformer for the Calculation of Leakage Inductance Using Eddy-Current Reaction Field

Ka Wai Eric Cheng, *Member, IEEE*

Department of Electrical Engineering, The Hong Kong Polytechnic University, Hung Hom, Hong Kong

The design of high-frequency power converter is very difficult because the leakage inductance of the transformer affects the performance. With consideration of the high-frequency eddy current, the flux linkage due to the eddy-current reaction field using a proposed summation calculation method is computed. The leakage inductance of a high-frequency transformer is therefore characterized. An optimum design method of the transformer can be obtained. Experimental results confirm the affectivity of the calculation method.

***Index Terms*—Inductor, power conversion, transformer.**

I. Introduction

HIGH-FREQUENCY power conversion requires a transformer for voltage stepping up and down. As the conversion frequency is now approaching megahertz, the design of the transformer must be handled with care. One of the typical examples is the forward converter; the existence of the leakage inductance reduces the output voltage [1]. For high-frequency resonant converter, the leakage inductance can be used as part of the resonant inductance [1], therefore the accurate calculation of the leakage inductance is necessary. A basic one-dimensional solution to the diffusion equations for high-frequency ac resistance has been demonstrated for the toroidal inductor with single strand [2]. For high-frequency operation, because of the eddy-current loss and proximity effect, multistranded windings are commonly used to reduce the loss for many practical engineers. Therefore, calculation of the leakage inductance with multilayer and multistranded windings is important. Simplified analysis for leakage inductance calculation [3], [4] for ring core has been reported where the eddy-current reaction field is neglected. Therefore, the analysis is not suitable for high-frequency operation. Few publications have reported on high-frequency transformer that is suitable for practical power converters. Also, the optimum design for the leakage inductance and its influence on the inductor size, number of strands, turn-pitch and number of layers are not explored in the past. In this paper, a model for the high-frequency transformer is proposed that is an extension of the method in [5]. Based on this model, the leakage inductance on multistranded and multiplayer winding is computed and can be applied at any frequency.

II. Computational Procedure

A. Model

A model for the multistranded and multiplayer winding of transformer is shown in Fig. 1. The model illustrates how a stranded wire of $M*M$ strands and N layers of winding can be formulated. The conductor is assumed to be square in cross section to make the calculation to be tractable. The stranded wire is also assumed to be evenly interleaved so that all the positions experience the same magnetic condition. Only one set of primary or secondary windings is shown. The other set of windings can be between the winding shown and the core. There are two components of the leakage inductance. One is frequency-independent components and the other is frequency dependent. The former is mainly due to the stored energy in the interlayer and inter-strand gaps. The latter is due to the flux crossing the winding space.

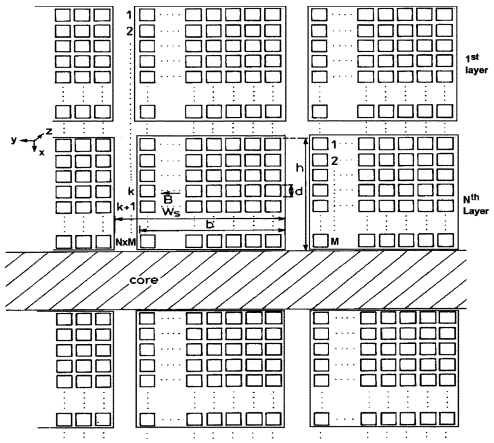

Fig. 1. Model of the stranded conductor wingings.

The frequency-independent component is simple for computation. The frequency-dependent component is the theme of the paper as it affects the performance of a transformer significantly and will be discussed in detail.

B. Development of the Computation

Under high-frequency operation, the distribution of the eddy current can be solved by a simultaneous solution of Ampere's law and Faraday's law

$$\nabla \times E = -\frac{dB}{dt} \tag{1}$$

$$E = \rho J \tag{2}$$

Digital Object Identifier 10.1109/TMAG.2005.846274

0018-9464/$20.00 © 2005 IEEE

Authorized licensed use limited to: Hong Kong Polytechnic University. Downloaded on July 14, 2009 at 03:15 from IEEE Xplore. Restrictions apply.

where ρ is the resistivity of the conductor and J is the current density and is z-directed, and B is y-directed. For single-frequency ω

$$\frac{dJ}{dx} = \frac{j\omega B}{\rho} \tag{3}$$

where ω is the frequency. Using Ampere's law, B at the kth row can be shown to be

$$B = \frac{\mu_o b}{W_s}\eta\left\{\overline{J}\eta h\left(\frac{k-1}{N}\right) + \int_o^x J dx\right\} \tag{4}$$

where η, is the internal packaging factor of the stranded conductor, $= Md/h$, μ_o is the permeability of free space, W_s is the turn pitch, and $\overline{J}$ is the average current density. If J_d is the current density in a strand at $x = d$, (3) and (4) gives

$$J_d = \overline{J}\alpha d\left\{\coth \alpha d + (k-1)\tanh\frac{\alpha d}{2}\right\} \tag{5}$$

where $\alpha = (j\omega\mu_o b\eta/\rho W_s)^2$. The voltage drop per unit length at $x = d$ in the kth row is the sum of the conduction drop due to (5) and the induced voltage due to the flux linkage resulted from (4). Because of perfect interleaving of the strands, the induced voltage across a strand is derived from the average of the voltages induced in a strand in each row. Therefore, for the ohmic voltage drop, the corresponding voltage is the average of the value of the ohmic voltage drop for all values of k in a layer q

$$V_r = \frac{1}{M}\sum_{k=(q-1)M+1}^{qM} \rho J_d. \tag{6}$$

For induced voltage drop, the induced voltage in kth row has an effect from each row below, i.e., from $k+1$ to NM. The total induced voltage is the average of the voltages induced in a strand in each layer. Hence

$$V_i = \frac{1}{M}\sum_{k=(q-1)M+1}^{qM}\sum_{k+1}^{NM} V_{i_k} \tag{7}$$

where V_{ik} is the induced voltage in the kth row and can be computed by

$$V_{i_k} = j\omega\int_0^d B dx. \tag{8}$$

It follows that the total voltage per unit length at qth layer is

$$V_{T_q} = \frac{1}{M}\sum_{k=(q-1)M+1}^{qM}\left(\overline{J}\alpha d\rho\left\{\coth\alpha d + (k-1)\tanh\frac{\alpha d}{2}\right\}\right) + \frac{1}{M}\sum_{k=(q-1)M+1}^{qM}\sum_{k+1}^{NM} 2\overline{J}\alpha d\rho\left(k-\frac{1}{2}\right)\tanh\alpha d. \tag{9}$$

The first portion on the right-hand side of (9) is due to the ohmic voltage drop and the second portion is due to the flux links all rows above the kth row at $\mathrm{x} = \mathrm{d}$. The total voltage across the winding is equal to the voltage drop of the leakage inductance. That is

$$\omega L_k = \frac{imag\left(\sum_{q=1}^{N} V_{T_q}\right)}{\overline{J}Nd^2M^2}. \tag{10}$$

It can be seen that the above equations (4)–(10) represent a one-dimensional computation of the B-field with reaction field being considered. The proposed computational method give an alternative way to calculate the leakage inductance as compared with finite element or analytical method.

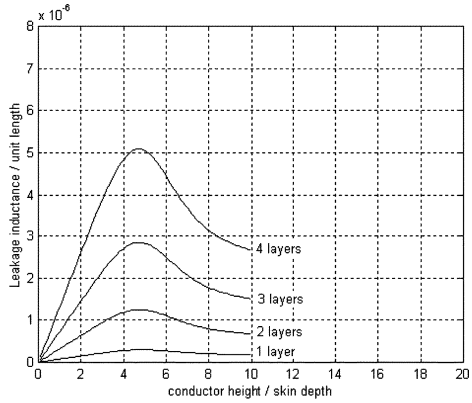

Fig. 2. Leakage inductance against conductor size—$\mathrm{Ws}' = 10$ and 16 strands.

C. Normalization

In order to make the simulation results be used in any frequency, a normalized method is proposed here. The strand conductor dimension d' can be expressed in term of skin depth, i.e., d/δ, where the skin depth is

$$\delta = \sqrt{\frac{2\rho}{\omega\mu_o}}. \tag{11}$$

Also, the αd term in (9) can be expressed as

$$\alpha d = \sqrt{j\frac{2b'\eta}{W_S'}}d' \tag{12}$$

where b' and W_S' are the normalized values for b/δ and Ws/δ respectively. The leakage inductance is independent of the current density by observing from (10) and (11). The other constants including q, M, N, and ρ are fixed and user-defined. Therefore, the computational results can be applied to any frequency. The following results will present all the dimensions in terms of skin depth. Users can denormalize by using the skin depth at any operational frequency.

III. Characteristics of the Leakage Inductance

The above methodology has been programmed and the results for a variation of layers and number of strands have been produced.

A. Leakage Inductance in Terms of Number of Layers

Figs. 2–5 show the leakage inductance against conductor (bundle size) with various numbers of layers. Each of the figures shows the different combinations of turn-pitches, ($Ws' = 10$

Authorized licensed use limited to: Hong Kong Polytechnic University. Downloaded on July 14, 2009 at 03:15 from IEEE Xplore. Restrictions apply.

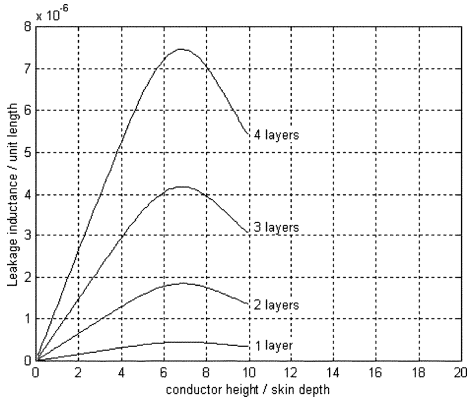

Fig. 3. Leakage inductance against conductor size—$\mathrm{Ws}' = 10$ and 49 strands.

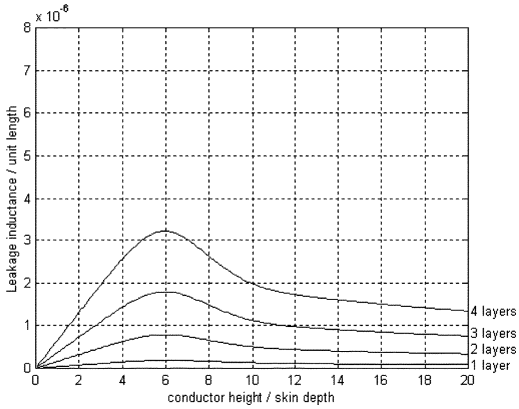

Fig. 4. Leakage inductance against conductor size—$\mathrm{Ws}' = 20$ and 16 strands.

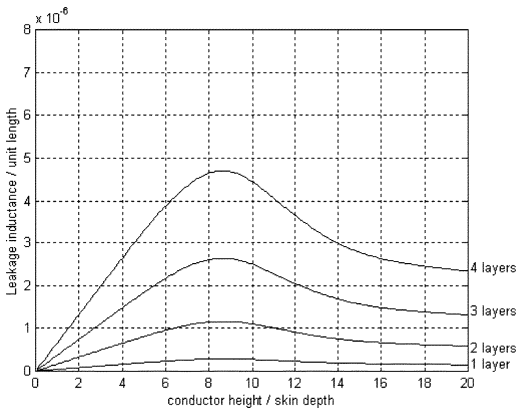

Fig. 5. Leakage inductance against conductor size—$\mathrm{Ws}' = 20$ and 49 strands.

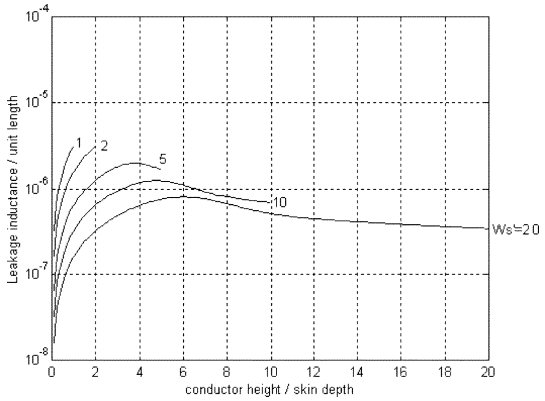

Fig. 6. Leakage inductance against conductor (bundle) size—2 layers and 16 strands.

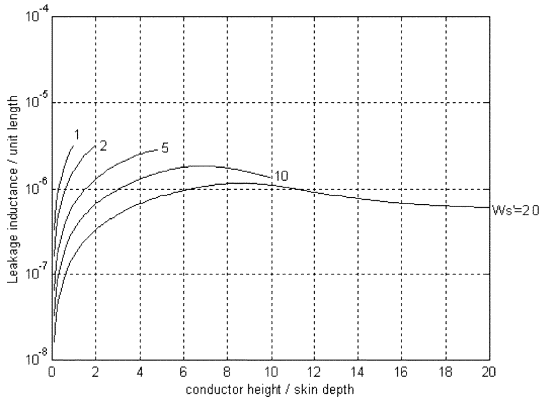

Fig. 7. Leakage inductance against conductor (bundle) size—2 layers and 49 strands.

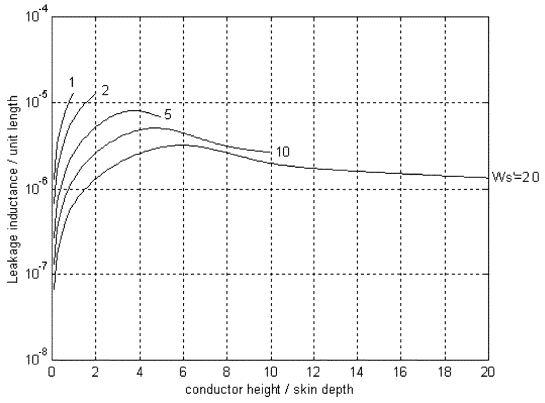

Fig. 8. Leakage inductance against conductor (bundle) size—4 layers and 16 strands.

and 20) and number of strands (16 and 49). The graphs in Figs. 2 and 3 break when conductor size reaches 10 because of the physical size that turn-pitch Ws' is only 10. It can be seen that as the number of layers increases, the leakage inductance increases.

There exists a crest value as the conductor size varies. This crest value changes with the number of strands and turn pitch. It can also be seen that as the number of strands increases, the crest value occurs at a larger value of conductor size, but the crest value is relatively independent of the number of layers for a fixed number of strands and turn pitch.

B. Leakage Inductance in Term of Turn Pitch

Figs. 6–9 show the leakage inductance for various normalized turn pitch Ws' (varies between 1 to 20). This turn pitch is a measure of how the packaging density of the turns affects the leakage inductance. The graph breaks for $\mathrm{Ws}' = 1$ to 10 because the physical condition that the bundle size cannot be greater than the turn pitches.

As the number of strands or the number of layers increases, the leakage inductance also increases. This is mainly because the number of strands and layers increase the eddy-current reaction field and hence increase the leakage inductance.

Authorized licensed use limited to: Hong Kong Polytechnic University. Downloaded on July 14, 2009 at 03:15 from IEEE Xplore. Restrictions apply.

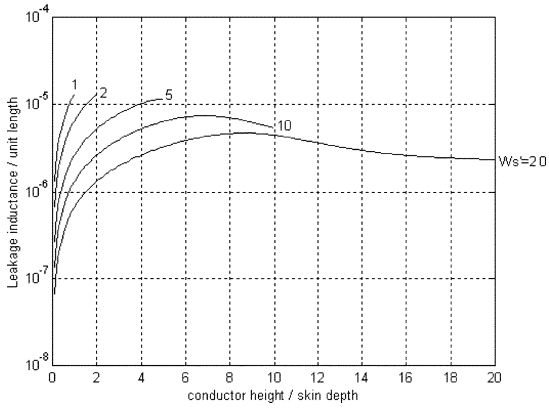

Fig. 9. Leakage inductance against conductor (bundle) size—4 layers and 49 strands.

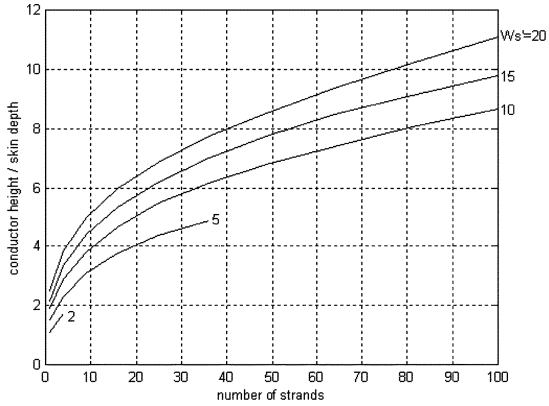

Fig. 10. Optimum crest value of leakage inductance against number of strands with various turn-pitches.

C. Optimum Characteristics of Leakage Inductance

The following conclusion can be drawn from the computed characteristics.

- For small conductor (bundle) size compared to turn-pitch, the leakage inductance is small.
- Leakage inductance increases with the number of layers and number of strands.
- Leakage inductance does not increase monotonically with conductor size, it has a maximum value with a certain conductor size.
- For large turn-pitch, such as $\mathrm{Ws}' = 20$, the leakage inductance reaches a fixed value when conductor size increases.

The optimum crest value of leakage inductance has been plotted in Fig. 10. This figure is the most important summary of the paper as it shows where the location of the peak value. Using this graph, the maximum value of leakage inductance can be obtained. This is usually for resonant power converter and transformer designs.

IV. Experimental Verification

The computed characteristics have been verified with experimental test. In order to examine the characteristics, high-frequency transformer with magnetizing inductance of 100 μH to 1 mH were constructed. The high-frequency transformers were tested from 10 kHz to 1 MHz. Construction and measurement

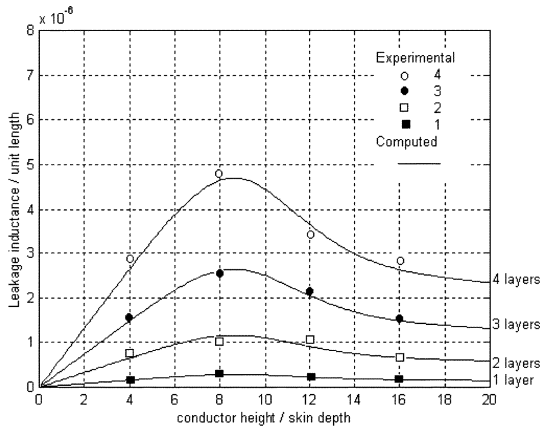

Fig. 11. Experimental results of the leakage inductance against conductor size.

of each transformer is needed for each data point. Fig. 11 shows a set of measurement of the leakage inductance characteristics. Sixteen transformers were needed for this verification. The leakage inductances were measured using the classical method of short-circuit tests with the HP impedance analyzer. Less than 10% error was obtained.

V. Conclusion

A generalized analysis of leakage inductance has been presented. The method is based on consideration of the eddy-current reaction field. Computed results show that there exist maximum values for the characteristics. Experimental results using N67-Rm12 cores were constructed to examine the calculation. Less than 10% error was obtained.

For the switched-mode power converter design, these maximum values of the characteristic curve must be avoided. For the resonant power conversion design where the leakage inductance is needed for the part of the resonance circuit, the optimum peak value can be used to reduce the size of the additional resonant inductor.

Acknowledgment

This work was supported by the Research Grants Committee of Hong Kong under Grant PolyU 5103/01E and the Research Committee of the Hong Kong Polytechnic University under Project number B-Q474.

References

[1] K. W. E. Cheng and P. D. Evans, "The unified theory of extended-period quasi-resonant converter," *IEE Proc.—Electr. Power Appl.*, vol. 147, no. 2, pp. 666–669, Mar. 2000.

[2] ——, "Calculation of winding losses in high frequency toroidal inductors using single strand conductors," *IEE Proc.—Electr. Power Appl.*, vol. 141, no. 2, pp. 52–62, Mar. 1994.

[3] W. G. Hurley and D. J. Wilcox, "Calculation of leakage inductance in transformer windings," *IEEE Trans. Power Electron.*, vol. 9, no. 1, pp. 121–126, Jan. 1994.

[4] P. N. Murgatroyd, "Calculation of proximity losses in multistranded conductor bunches," *IEE Proc. A*, vol. 136, no. 3, pp. 115–120, 1989.

[5] J. A. Ferreira, "Analytical computation of AC resistance of round and rectangular litz wire windings," *IEE Proc. B*, vol. 139, no. 1, pp. 21–28, 1992.

Manuscript received June 8, 2004.

Authorized licensed use limited to: Hong Kong Polytechnic University. Downloaded on July 14, 2009 at 03:15 from IEEE Xplore. Restrictions apply.